AbaM Regulates Quorum Sensing, Biofilm Formation and Virulence in *Acinetobacter baumannii*

Mario López-Martín[1], Jean-Frédéric Dubern[1], Morgan R. Alexander[2], Paul Williams[1]*

[1]Biodiscovery Institute and School of Life Sciences, University of Nottingham, Nottingham, United Kingdom.

[2]Advanced Materials and Healthcare Technologies, School of Pharmacy, University of Nottingham, Nottingham, United Kingdom

Running title: AbaM and quorum sensing in *Acinetobacter*

Keywords: *Acinetobacter*, quorum sensing, *N*-acylhomoserine lactones, RsaM, virulence, biofilms

Corresponding author email: paul.williams@nottingham.ac.uk

ABSTRACT

Acinetobacter baumannii possesses a single divergent *luxR*/*luxI*-type quorum sensing (QS) locus named *abaR*/*abaI*. This locus also contains a third gene located between *abaR* and *abaI* which we term *abaM* that codes for an uncharacterized member of the RsaM protein family known to regulate *N*-acylhomoserine lactone (AHL) dependent QS in other β- and γ-proteobacteria. Here we show that disruption of *abaM* via a T26 insertion in *A. baumannii* strain AB5075 resulted in increased production of *N*-(3-hydroxydodecanoyl)-L-homoserine lactone (OHC12) and enhanced surface motility and biofilm formation. In contrast to the wild type and *abaI*::T26 mutant, the virulence of the *abaM::*T26 mutant was completely attenuated in a *Galleria mellonella* infection model. Transcriptomic analysis of the *abaM*::T26 mutant revealed that AbaM differentially regulates at least 76 genes including the *csu* pilus operon and the acinetin 505 lipopeptide biosynthetic operon, that are involved in surface adherence, biofilm formation and virulence. A comparison of the wild type, *abaM*::T26 and *abaI::*T26 transcriptomes, indicates that AbaM regulates ~21% of the QS regulon including the *csu* operon. Moreover, the QS genes (*abaI*/*abaR*) were among the most upregulated in the *abaM*::T26 mutant. *A. baumannii lux*-based *abaM* reporter gene fusions revealed that *abaM* expression is positively regulated by QS but negatively auto-regulated. Overall, the data presented in this work demonstrates that AbaM plays a central role in regulating *A. baumannii* QS, virulence, surface motility and biofilm formation.

43 **IMPORTANCE**

44 *Acinetobacter baumanni* is a multi-antibiotic resistant pathogen of global healthcare
45 importance. Understanding *Acinetobacter* virulence gene regulation could aid the
46 development of novel anti-infective strategies. In *A. baumannii,* the *abaR* and *abaI* genes
47 that code for the receptor and synthase components of an *N*-acylhomoserine (AHL) lactone-
48 dependent quorum sensing system (QS) are separated by *abaM.* Here we show that
49 although mutation of *abaM* increased AHL production, surface motility and biofilm
50 development, it resulted in the attenuation of virulence. AbaM was found to control both
51 QS-dependent and QS-independent genes. The significance of this work lies in the
52 identification of AbaM, an RsaM ortholog known to control virulence in plant pathogens, as
53 a modulator of virulence in a human pathogen.

54

55

56

57

58

59 **INTRODUCTION**

60 *Acinetobacter baumannii* is a Gram-negative opportunistic nosocomial pathogen that causes
61 a wide range of infections in humans, most commonly pneumonia, but also bacteremia,
62 skin, soft tissue and urinary tract infections, meningitis and endocarditis (1). The rise of
63 multi-drug resistant strains has limited the treatment options for this pathogen which has
64 become a major threat to hospital patients worldwide (2). Indeed, the WHO classified *A.*
65 *baumannii* as a critical pathogen for which new antibiotics are urgently required (3). For this
66 reason, a better understanding of the virulence of *A. baumannii* should aid the development
67 of new therapeutic strategies for preventing and treating *Acinetobacter* infections. Several
68 virulence factors and regulators involved in *A. baumannii* pathogenesis have been
69 characterized to date. These include outer membrane proteins (e.g. OmpA), pili, capsular
70 polysaccharide, iron acquisition systems, outer membrane vesicles, secretion systems and
71 phospholipases (4–9), as well as regulators such as H-NS and two component systems (10–
72 13). Some *A. baumannii* strains also undergo phase variation where opaque colony variants
73 exhibit greater motility and virulence but reduced biofilm formation compared with the
74 translucent variants (11). A detailed review of *A. baumannii* virulence can be found in Morris
75 *et al*, 2019 (14).

76

77 One well-established mechanism of virulence gene regulation in diverse pathogens is
78 quorum sensing (QS) (15). This cell-cell communication system is employed by bacteria to
79 coordinate the expression of specific genes as a function of population density. QS is
80 mediated via the synthesis, release and detection of diffusible signalling molecules such as
81 the *N*-acyl-homoserine lactones (AHLs) (16). *A. baumannii* and related pathogenic
82 *Acinetobacter* spp. possess a LuxR/LuxI QS system, consisting of an AHL synthase (AbaI) and

83 a transcriptional regulator (AbaR) that is activated on binding an AHL. Most pathogenic
84 *Acinetobacter* spp. produce AHLs with acyl side chains of 10 to 12 carbons length with *N*-(3-
85 hydroxydodecanoyl)-L-homoserine lactone (OHC12) being most commonly encountered.
86 Many strains are however capable of producing other AHLs (17). Several reports have linked
87 QS to biofilm formation and surface motility (18–20) while others have suggested that it
88 plays a role in virulence in a strain and animal model dependent manner (21, 22). However,
89 our current knowledge of the role of QS in the virulence of pathogenic *Acinetobacter* spp. is
90 limited.
91
92 Located adjacent to the *abaI* gene in *Acinetobacter* there is an ortholog of the RsaM protein
93 family. These are found in diverse β- and γ-proteobacteria, including *Burkholderia* spp.,
94 *Pseudomonas fuscovaginae, Halothiobacillus neapolitanus* and *Acidithiobacillus ferrooxidans*
95 (23). The first ortholog to be characterized was RsaM in the plant pathogen *P. fuscovaginae*.
96 This was shown to negatively regulate AHL production and was required for full virulence in
97 rice plants (24). Transcriptomic analysis revealed that RsaM partially regulates the QS
98 regulon, as well as modulating the expression of diverse genes in a QS-independent manner
99 (25). Similarly, TofM, the RsaM ortholog found in *Burkholderia glumae*, represses AHL
100 production while positively regulating toxoflavin and virulence in rice (26). The two RsaM
101 orthologs present in *Burkholderia thailandensis* are both negatively auto-regulated while
102 being positively controlled by their cognate QS systems (27). In *Burkholderia cenocepacia*
103 H111, *Bc*RsaM downregulates AHL biosynthesis and modulates swarming motility, biofilm
104 formation, protease and siderophore production (28). Structural and biochemical analysis of
105 *Bc*RsaM showed that it forms dimers in solution and does not appear to bind DNA or AHLs,

106 suggesting that RsaM family proteins act as post-transcriptional or post-translational
107 regulators (23).
108
109 RsaM orthologs clearly play a central role in the regulation of QS-dependent and QS-
110 independent gene expression and virulence in plant pathogens. Here we investigated the
111 role and regulation of *abaM* in *A. baumannii* AB5075, a comparatively recently isolated
112 multi-antibiotic resistant, hypervirulent strain (29). We show that AbaM, in the opaque
113 variant of *A. baumanni* 5075, controls AHL production, surface motility and biofilm
114 formation and is required for virulence in a *Galleria mellonella* infection model. QS
115 positively regulates *abaM* expression which is turn is negatively autoregulated.
116 Transcriptomic analysis of the *abaM* and *abaI* mutants indicate that the AbaM and QS
117 regulons overlap. These data are consistent with a central role for AbaM in regulating gene
118 expression and the pathobiology of *A. baumannii*.
119

120 **RESULTS**

121 **Organization of the QS locus in *A. baumannii* 5075.** The genome of *A. baumannii* AB5075
122 possesses a single QS locus comprised of two divergently transcribed genes: an AHL
123 synthase (*abaI/ABUW_3776/ABUW_RS18385*) and a response regulator
124 (*abaR/ABUW_3774/ ABUW_RS18375*) gene. Between *abaR* and *abaI* a third gene is located
125 which here we term *abaM* (*ABUW_3775*) (**Fig. 1A**). The chromosomal organization of these
126 three QS genes is well conserved among *Acinetobacter* spp (**Fig. S1**). Despite the location of
127 *abaM* adjacent to *abaI* and transcribed in the same direction, AbaM has only low (~20-30 %)
128 sequence identity to orthologs present in *Pseudomonas fuscovaginae* and *Burkholderia spp*
129 (**Fig. 1B**). However, it retains the well-conserved regions shared by other RsaM orthologues,
130 including most of the protein secondary structural elements and the characteristic
131 hydrophobic core cluster, consisting of four tryptophan residues (Trp60, Trp75, Trp77 and
132 Trp125) (23).

133

134 **AHL production is enhanced in an *abaM* mutant** AHL production in the opaque variants of
135 the AB5075 wild type, *abaM*::T26 and *abaI*::T26 mutants respectively was quantified via LC
136 MS/MS during growth under static conditions since it appears to be enhanced by surface
137 attachment in other *A. baumannii* strains (30). OHC12 (**Fig. 2A**) was the major AHL produced
138 by AB5075 under these conditions. Compared with the wild type, the *abaM*::T26 mutant
139 produced significantly greater amounts of OHC12 at each time point (between 100 and
140 875-fold difference) sampled (**Fig. 2B**). *N*-(3-hydroxydecanoyl)-L-homoserine (OHC10), was
141 also detected at much lower concentrations in the *abaM*::T26 mutant throughout growth,
142 but only in the 24 h sample in the wild type (**Fig. 2C**). No AHLs were detected in any of the

143 *abaI*::T26 samples (**Fig. 2B and C**). These data suggest that AbaM is a negative regulator of
144 AHL production.

145 **Contribution of QS and *abaM* to surface motility, biofilm formation and virulence.** The
146 surface motility of all three strains on 0.3% Eiken agar LS-LB plates was examined.
147 Compared with the wild-type (59.6 ± 0.7 mm), the *abaI*::T26 mutant exhibited significantly
148 reduced (36.5 ± 1.4 mm) whereas the *abaM*::T26 mutant was significantly more motile (76.7
149 ± 2.4 mm) (**Fig. 3A**). The provision of exogenous OHC12 increased the surface motility of
150 both wild type and *abaI* mutant to a similar level to that of the *abaM* mutant (**Fig. S2A**)

151 The ability of AB5075, *abaI*::T26 and *abaM*::T26 to attach to abiotic surfaces was evaluated
152 on propylene tubes. The *abaM* mutant formed ~3 fold more biofilm than the wild-type (**Fig.**
153 **3B**). Under these growth conditions, the biofilm produced by the *abaI* mutant (opaque
154 variant; **Fig. 3B**) was not significantly different from than the wild type but increased
155 following the exogenous provision of OHC12 (**Fig. S2B**).

156 The contribution of *abaM* and QS to AB7075 virulence was assessed using a
157 *G. mellonella* larvae infection model (**Fig. 3C**). No differences in killing were observed
158 between the wild-type and the *abaI*::T26 mutant when injecting either
159 2×10^4 or 2×10^5 CFU/larva. However, the *abaM*::T26 mutant was significantly less virulent
160 than the parental strain. Larvae injected with 2×10^5 CFU of the *abaM*::T26 mutant also
161 showed a lower death rate than the larvae injected with 2×10^4 CFU of the wild-type or the
162 *abaI*::T26 mutant. Exogenously supplied OHC12 did not affect the virulence of the wild type
163 (**Fig. S2C**).

164 Overall, these results suggest that *abaM* is a negative regulator of surface motility and
165 biofilm formation and required for full virulence in *G. mellonella*.

166 **Genetic complementation of the *abaM* mutant phenotypes.** Complementation of the
167 *abaM*::T26 mutant with the *abaM* gene in *trans* (pMQ_*abaM*) restored surface motility
168 (**Fig.S3A**), biofilm formation (**Fig. S3B**) and reduced both OHC12 and OHC10 production by
169 approximately 50% (**Fig. S3C and D**). However, complementation of the *abaM* mutation did
170 not restore *abaM*::T26 virulence to wild-type (**Fig. S3E**).

171 **Transcriptomic analysis of *abaI*::T26 and *abaM*::T26.** To characterize the AbaM and QS
172 regulon of *A. baumannii* AB5075, we performed transcriptomic profiling of AB5075 in
173 comparison with the *abaM*::T26 and *abaI*::T26 mutants using RNA sequencing (RNA-seq),
174 which was then validated for two key target genes via quantitative real-time PCR. For these
175 analyses we used total RNA extractions from cells grown for 18 h in static conditions when
176 maximum OHC12 levels are produced by the *abaM* mutant (**Fig. 2**).

177 When compared with the wild-type strain, 88 genes were upregulated and 9 downregulated
178 in the *abaI*::T26 mutant, while 52 were upregulated and 24 downregulated in the
179 *abaM*::T26 mutant ($\log_2$(fold change) ≥ 1; **Fig.4** and **Tables S3** and **S4**). Moreover, 21 of the
180 upregulated genes were shared between *abaI*::T26 and *abaM*::T26 (**Fig. 4, Tables S3** and
181 **S4**), while none of the downregulated genes were co-regulated. Among the genes
182 upregulated in both mutants there were all the genes of the *csu* operon, a putative TetR
183 family transcriptional regulator (*ABUW_1486/ABUW_RS07245)* located immediately
184 upstream of the *csu* operon as well as genes coding for a flavohemoprotein, an

185 uncharacterized transcriptional regulator, a thermonuclease, a sulfate permease, a toxic
186 anion resistance protein and 7 hypothetical proteins (**Tables S3 and S4**).

187 Moreover, genes of the biosynthetic operon involved in the synthesis of acinetin 505, the
188 QS response regulator, *abaR* and the AHL synthase *abaI* were both upregulated in the
189 *abaM*::T26 mutant, which also differentially expressed genes encoding for proteins involved
190 in the stress response, iron-acquisition, diverse metabolism and energy production,
191 chaperones, protein folding and antibiotic resistance e.g. class D beta-lactamase OXA-23
192 involved in resistance to carbapenems (**Table S4**). Similarly, differentially regulated genes in
193 the *abaI* mutant included diverse metabolic and energy production-related genes, as well as
194 diverse genes coding for transcriptional regulators, stress response-related proteins and
195 membrane transport proteins (**Tables S3)**.

196 To validate the transcriptomic data, qPCR was performed with the same RNA samples used
197 in the RNA-seq for the *csuA/B* and the *ABUW_3773* (the first gene of the acinetin 505
198 biosynthetic operon) genes (**Fig. 5**). When compared with the wild-type, the data obtained
199 showed a significant increase in *csuA/B* expression in both the *abaI*::T26 and *abaM*::T26
200 mutants, while *ABUW_3773* expression was significantly higher only in the *abaM*::T26
201 mutant. These results correlate with the data obtained from the RNA-seq experiments.

202 **Regulation of *abaM*.** To further elucidate the regulation of *abaM* expression, an *abaM*
203 promoter – *luxCDABE* operon fusion was constructed. This was introduced via a miniTn*7*
204 transposon into AB5075 and both *abaI*::T26 and *abaM*::T26 mutants, and the activity of the
205 predicted promoter was measured by luminescence output in the presence or absence of
206 OHC12. The activity of the *abaM* promoter significantly varied between the strains. In the

207 *abaM*::T26, luminescence was approximately 40% higher than in the wild-type, while the
208 *abaI*::T26 mutant showed a 75% reduction when compared with the parental strain (**Fig.**
209 **6A**). Moreover, exogenous provision of OHC12 increased the *abaM* promoter activity in all
210 three strains (**Fig. 6B**). Similarly, **Fig. 6C** shows that expression of an *abaI*::*lux* promoter
211 fusion which is reduced in the *abaI* mutant compared with the wild type strain, is strongly
212 stimulated by OHC12. These data suggest that *abaM* expression is negatively autoregulated
213 but, in common with *abaI* is positively regulated by QS which in turn is negatively controlled
214 via AbaM (**Fig. 7**).

215 **DISCUSSION**

216 In this study we have established that the RsaM ortholog, AbaM plays a major role in
217 regulating QS-dependent and QS-independent genes in *A. baumannii* 5075. Disruption of
218 *abaM* substantially increased AHL production, indicating that AbaM negatively regulates
219 AHL biosynthesis. In *A. baumannii* 5075, the concentration of OHC12 produced was very low
220 (< 1 nM), suggesting that, at least under the static growth conditions used in this study,
221 AbaM exerts tight control over QS. This raises the question of when and under what
222 conditions QS is active in AB5075, especially since the half-maximal responses for LuxR
223 proteins activated by long chain AHLs is in the 5-10 nM range (31). In *A. baumannii*, the QS
224 locus has an *RXI* topological arrangement previously described in other bacteria, where the
225 *X* gene between the QS regulator (*R*) and the synthase (*I*) genes is a negative regulator of
226 QS. Examples of three different classes of X include *rsaL*, *rsaM* and *mupX* (32). In this
227 context, AbaM appears to behave similarly to RsaL in the *Pseudomonas aeruginosa*
228 *lasR/rsaL/lasI* QS system, despite their functional and structural differences. The *rsaL* gene

229 which is divergent to *lasI* is positively regulated by LasR and antagonizes LasR-mediated
230 activation of *lasI* so counteracting the QS positive feedback autoinduction and providing
231 AHL homeostasis (33). This type of regulatory circuit (**Fig. 7**), termed an incoherent feed
232 forward loop (IFFL) in contrast to simple feed forward loops, can display complex behaviours
233 that include stabilization of output signals and bounded output which ensures robustness
234 against fluctuations in the input signal levels (32, 34). Hence the large increase in AHL
235 production following deletion of *abaM*, *rsaL* and *rsaM* genes that result in less virulent
236 mutants is indicative of the importance of a stabilizing negative regulatory pathway in AHL-
237 dependent QS systems (32, 34).

238 Consistent with this model, *abaM* expression was found to be negatively auto-regulated but
239 positively regulated by QS. *In silico* analysis of the DNA sequence between *abaR* and *abaI*
240 using Bprom (www.softberry.com) and BDGP (www.fruitfly.org) as well as our RNAseq data
241 all predict the presence of putative -10 and -35 regions for *abaI* and *abaM* respectively
242 suggesting that these genes are not co-transcribed. Similar findings have been reported for
243 *rsaM1* and *rsaM2* from *Burkholderia thailandensis* (27). Reverse transcriptase (RT)-PCR (**Fig.**
244 **S4**) confirm that *abaM* and *abaI* in *A. baumannii* A5075 do not form an operon. Moreover,
245 the *abaM* gene has a predicted *lux*-box (CTGGTTAAATATAACAG) 68 bp upstream of the start
246 codon and 178 bp downstream of the -35 and -10 promoter elements. This *lux*-box is similar
247 to those found upstream of *abaI* (CTGTAAATTCTTACAG) in both *A. baumannii* 5075 and *A.*
248 *nosocomialis* M2. These results are consistent with an IFFL circuit although further work will
249 be required to fully characterize its properties and control of genes co-regulated by QS and
250 AbaM.
251

252 Phenotypic characterization of the *A. baumanni abaM* mutant revealed enhanced surface
253 motility and biofilm formation but reduced virulence compared with the wild type. Previous
254 studies have shown that *rsaM* orthologues are required for full virulence in plants (24, 26),
255 but this is, to the best of our knowledge, the first time that an *rsaM*-like gene has been
256 reported to be required for full virulence in a human pathogen albeit in an insect infection
257 model. The contribution of *Bc*rsaM in *B. cenocepacia* to swarming motility and biofilm
258 formation has also been reported (28). However, deletion of *bcrsaM* reduced both
259 swarming and surface attachment, the opposite to that observed for the *abaM* mutant.
260 Interestingly, both biofilm formation and surface motility in *Acinetobacter* have been
261 associated with increased virulence (10, 35).
262
263 Genetic complementation of the *abaM* mutant was achieved for surface motility, biofilm
264 formation and AHL production but not for virulence in *Galleria mellonella.* Similar
265 observations have been previously reported for other *abaM* orthologues, most notably
266 *tofM* (26) and *bcrsaM* (28), leading to the suggestion that RsaM-like proteins may be *cis*-
267 acting regulators (23).
268
269 To further define the role of QS in *A. baumannii* 5075, phenotypic characterization of the
270 AHL synthase mutant, *abaI*::T26, was performed. The mutant did not produce any
271 detectable AHLs, consistent with previous studies and bioinformatic analysis indicating that
272 *A. baumannii* 5075 possesses a single QS locus that is responsible for AHL production (18,
273 36). Similarly, disruption of *abaI* negatively affected surface motility and responded to
274 exogenous 3OHC12, as previously noted for other *Acinetobacter* strains/species (20). In
275 AB5075, biofilm formation in the opaque variant of the *abaI*::T26 mutant was not

276 significantly different from with wild type. However, it increased well above wild type in
277 response to exogenous OHC12. consistent with other work on the *Acinetobacter* AHL
278 synthase (18, 37). Previous studies on QS and biofilm formation in *Acinetobacter* have been
279 performed with strains that were, in contrast to AB5075, either not phase variable or not
280 known to be phase variable. Since the experiments performed in this study were all carried
281 out with the opaque *Acinetobacter* variant, we also investigated biofilm formation by the
282 translucent variant. **Fig S5** shows that the translucent variant produced less biofilm that the
283 wild type. However, biofilm formation increased for both opaque and translucent variants
284 in response to exogenous OHC12. Furthermore, our results suggest that QS does not play
285 an important role in virulence in the *G. mellonella*. While this is not unprecedented (38), the
286 role of *Acinetobacter* QS in virulence is still not well defined, and other studies suggest that
287 QS may play an important role, depending on the strain and infection model used (21, 22).
288 Overall, our data suggest that for strain AB5075, QS is important in surface motility and
289 biofilm formation, but not virulence. However, further work is required to fully elucidate the
290 role of QS in the pathogenesis of *Acinetobacter* infection and any cross-talk with other
291 regulatory networks.

292 Here we performed RNAseq on *A. baumannii* AB5075 grown in static conditions where AHL
293 production was elevated in order to identify genes regulated via AbaM and QS and likely to
294 be involved in surface attachment and biofilm formation. A comparison of the genes
295 differentially expressed in the *abaM* and *abaI* mutants with the wildtype revealed that
296 AbaM has both QS-dependent (~22% of the QS regulon) and QS independent gene targets.
297 A similar overlap has been noted for the RsaM regulon and its cognate QS system in *P.*
298 *fuscovaginae* (25). Among the most upregulated genes in both *abaI* and *abaM* mutants

299 when compared with the wild-type were those belonging to the *csu* operon (*ABUW_1487-*
300 *ABUW_1492/ABUW_RS07250-ABUW_RS07275*). This operon encodes the proteins
301 responsible for the synthesis of the Csu pilus, a type I chaperone-usher pilus involved in
302 attachment and biofilm formation (39–41). Moreover, the *abaM*::T26 mutant also showed
303 higher expression of some genes of the acinetin 505 biosynthetic operon, which has also
304 been linked to biofilm formation in *A. baumannii* ATCC17978 (42).

305 A previous comparison of the transcriptomes of the multi-drug resistant clinical *A.*
306 *baumanni* strain 863 with an isogenic *abaI* deletion mutant highlighted the differential
307 regulation of 352 genes involved in carbon source metabolism, energy production, stress
308 response and translation (49). However, apart from *abaI*, no other common differentially
309 regulated genes could be identified when the A5075 *abaI* and the 863 *abaI* mutant
310 transcriptomes are compared. This may be because of the different strains and growth
311 conditions and sampling times used. In addition, the *abaI* mutant reported by Ng et al (49)
312 exhibited a growth defect (49). This raises the possibility of a secondary mutation
313 contributing to the transcriptome data which was not validated by chemical or genetic
314 complementation with OHC12 or *abaI* respectively.

315 The work described here establishes that AbaM plays a central role in regulating QS, surface
316 motility, biofilm formation and virulence. The apparently contradictory regulatory impact of
317 *abaM* and *abaI* mutations that result in either increased or no AHL production respectively
318 on the expression of genes such as the *csu* cluster can be explained as follows. In an *abaI*
319 mutant (no AHLs), *abaM* expression is reduced and hence *csu* expression is increased. In an
320 *abaM* mutant *csu* expression is also increased as AbaM is absent (**Fig. 7**). Further work will

321 be required to elucidate the biochemical function and mechanism of action of AbaM and
322 the RsaM protein family in general.
323

324 ## MATERIALS AND METHODS

325 **Strains and growth conditions.** The strains and plasmids used are listed in **Table S1.** *A.*
326 *baumannii* AB5075 (29) and the isogenic *abaI*::T26 and *abaM*::T26 mutants were obtained
327 from the transposon library available from the University of Washington (44). *A. baumannii*
328 was routinely grown in low-sodium chloride (5g/L) lysogeny broth (LS-LB). OHC12 was
329 synthesized as described before (46). The opaque and translucent phases of the wild type,
330 and mutants were separated as described by Tipton *et al* (11) after growth on phase-
331 observation LB (PO-LB) plates and observation of colonies under light microscopy using
332 oblique indirect illumination.

333 **Construction of a genetically complemented *abaM*::T26 strain.** Plasmid pMQ557M (**Table**
334 **S1**) was obtained by digesting pMQ557 with *Pml*I (to remove the genes required for yeast
335 replication) and re-ligating the resulting large linear product. The *abaM* gene plus 768 bp
336 from its upstream region (containing the predicted native promoter) were amplified by PCR
337 using primers listed in **Table S2**. The PCR fragments were digested with *Bam*HI and *Kpn*I and
338 ligated in the multiple cloning site (MCS) of both pMQpMQ557M and introduced into
339 *abaM*::T26 by electroporation. The stability of the vector pMQ557M and *abaM*
340 complementing plasmid pMQ_*abaM* in both A5075 and the *abaM* mutant mutant were
341 confirmed by repeated daily subculture and plating out on LB agar with and without
342 hygromycin (125µg/ml) to determine viable counts as cfu/ml (**Fig. S6**).

343 **Construction of *abaM::luxCDABE* and *abaI::luxCDABE* promoter fusions.** The *abaR* gene
344 and the intergenic region between *abaR* and *abaM* (for the *abaM* fusion) or the region
345 between *abaR* and the *abaI* (for the *abaI* fusion) were amplified by PCR and ligated in
346 pGEM®-T Easy using the pGEM®-T Easy Vector System (Promega). The resulting plasmids
347 and the promoterless *luxCDABE* operon were digested with *Kpn*I and *Bam*HI and ligated in
348 order to introduce the *lux* operon downstream of the predicted promoter of *abaM* or *abaI*.
349 These constructs were transferred into the MCS of the miniTn*7*T in pUC18T-miniTn*7*T-Hyg^R
350 plasmid (**Table S1**) after digesting with *Not*I and *Pst*I and ligating the corresponding
351 fragments.

352 MiniTn*7*T-based constructs were inserted into *A. baumannii* through four-parental
353 conjugation. Briefly, PBS-washed overnight cultures of the *E. coli* DH5α donor strain
354 (containing pUC18T-mini-Tn*7*T_Hyg^R_*abaR*_P*abaM*::*lux* or the pUC18T-mini-
355 Tn*7*T_Hyg^R_*abaR*_P*abaI*::*lux*), the *E. coli* DH5α helper strain (containing pUX-B13), the *E. coli*
356 DH5α mobilizable strain (containing pRK600) and the *A. baumanii* recipient strain were
357 mixed in a 1:1:1:1 ratio and grown on LB agar prior to counterselection with hygromycin
358 (125 µg/ml for miniTn*7* selection) and gentamicin (100 µg/ml).

359 The miniTn*7* transposon (45) carrying the *abaM* promoter-*lux* operon fusion was inserted
360 into *A. baumannii* AB5075 and the isogenic *abaI*::T26 and *abaM*::T26 mutants; while the
361 *abaI* promoter-*lux* fusion was inserted into AB5075 and the isogenic *abaI*:T26 mutant.
362 Bioluminescence output from the reporter fusions as a function of bacterial growth was
363 quantified using an Infinite 200 PRO (Tecan Diagnostics) plate-reader over 24 h and OD600
364 and relative light units RLUs were recorded every 30 min. When required OHC12 was added
365 at 200 nM unless otherwise stated.

366 **Biofilm assays.** Strains to be tested were inoculated into 1.5 ml polypropylene
367 microcentrifuge tubes in LS-LB with or without OHC12 and incubated under static conditions
368 at 37°C for 24 h. Biofilms were quantified by staining with 0.25% crystal violet, extracting
369 with ethanol and recording the absorbance at A_{585}.

370 **Surface motility assays.** Surface motility was quantified as previously described (11) on LS-
371 LB plates with or without OHC12 and containing 0.3% Eiken agar. Plates were incubated at
372 30°C for 16 h.

373 **AHL extraction and detection.** Cell-free supernatants from cultures grown in LS-LB under
374 static conditions at 37°C were sterile-filtered and extracted with acidified ethyl acetate.
375 Extracts were evaporated to dryness and subjected to by liquid chromatography with
376 tandem mass spectrometry (LC-MS/MS) as previously described (46).

377 ***G. mellonella* killing assays.** *G. mellonella* larvae (Trularv™) were obtained from
378 BioSystems Technology Ltd, U.K. Assays were performed as described previously (11).
379 Briefly, *Acinetobacter* (2×10^4 or 2×10^5 cfu) were injected into the larval hemolymph,
380 incubated at 37°C and the larvae monitored for viability. At least 10 larvae were used for
381 each strain and assay.

382 **Total RNA extraction and RNA-seq.** Bacteria were cultured in LS-LB under static conditions
383 at 37°C for 18h. Cells were resuspended in RNAprotect (Qiagen) prior to extracting total
384 RNA using an RNeasy minikit (QiAgen). After treatment with DNA-free (Invitrogen) the
385 absence of DNA contamination was conformed using by PCR and the quality and quantity of
386 the RNA samples was established using a 2100 Bioanalyzer (Agilent). Samples were sent for
387 150 bp paired-end sequencing via an Illumina platform and bioinformatic analysis, to

388 NovoGene (Hong Kong, China). The data have been deposited in NCBI's Gene Expression
389 Omnibus (50) and are accessible through GEO Series accession number GSE151925
390 (https://www.ncbi.nlm.nih.gov/geo/query/acc.cgi?acc=GSE151925; token for reviewers:
391 **wxqxkwygphkbliv**).

392 **Quantitative real-time PCR (qPCR).** Complementary DNA (cDNA) synthesis and qPCR were
393 carried out using LunaScript RT Supermix and Luna Universal qPCR Master Mix (New
394 England BioLabs), respectively. The oligonucleotides used for qPCR are listed in **Table S2** and
395 qPCR was carried out in triplicate using a 7500 Real-Time PCR System (Thermofisher).
396 Negative controls lacking template or RNA incubated without reverse transcriptase were
397 included. The housekeeping gene *rpoB* was used as endogenous control for normalization.
398

399 **Reverse transcription PCR (RT_PCR)**. cDNA was amplified using Q5 High-Fidelity polymerase
400 (New England Biolabs) using specific primers annealing in the coding region of each gene.
401 Genomic DNA, extracted using DNeasy Blood and Tissue kit (QIAgen), was used as a positive
402 control. The PCR products were run in a 1.5% agarose electrophoresis gel before imaging
403 under UV light using a Gel Doc XR+ Imager (Bio-Rad).

404 **ACKNOWLEDGEMENTS**

405 We thank Nigel M. Halliday for AHL quantification and Alex Truman for AHL synthesis,
406 Robert M.Q. Shanks (University of Pittsburgh) for kindly providing the pMQ557 plasmid and
407 Prof. Philip N. Rather from Emory University for his guidance and advice on *Acinetobacter*
408 phase variation. This work was supported via Wellcome Trust joint senior investigator

409 awards to MRA and PW (grant nos. 103882 and 103884). MLM was supported by a
410 University of Nottingham postgraduate doctoral studentship.

411 **REFERENCES**

412 1. Peleg AY, Seifert H, Paterson DL. 2008. *Acinetobacter baumannii*: Emergence of a
413 successful pathogen. Clin Microbiol Rev 21:538–582.
414 2. Lin M-F, Lan C-Y. 2014. Antimicrobial resistance in *Acinetobacter baumannii*: From
415 bench to bedside. World J Clin cases 2:787–814.
416 3. World Health Organization. 2017. WHO publishes list of bacteria for which new
417 antibiotics are urgently needed. Saudi Med J 38(4): 444–445.
418 4. Gaddy JA, Tomaras AP, Actis LA. 2009. The *Acinetobacter baumannii* 19606 OmpA
419 protein plays a role in biofilm formation on abiotic surfaces and in the interaction of
420 this pathogen with eukaryotic cells. Infect Immun 77:3150–3160.
421 5. Russo TA, Luke NR, Beanan JM, Olson R, Sauberan SL, MacDonald U, Schultz LW,
422 Umland TC, Campagnari AA. 2010. The K1 capsular polysaccharide of *Acinetobacter*
423 *baumannii* strain 307-0294 is a major virulence factor. Infect Immun 78:3993–4000.
424 6. Jin JS, Kwon S-O, Moon DC, Gurung M, Lee JH, Kim S Il, Lee JC. 2011. *Acinetobacter*
425 *baumannii* secretes cytotoxic outer membrane protein a via outer membrane
426 vesicles. PLoS One 6:e17027.
427 7. Runci F, Gentile V, Frangipani E, Rampioni G, Leoni L, Lucidi M, Visaggio D, Harris G,
428 Chen W, Stahl J, Averhoff B, Visca P. 2019. Contribution of active iron uptake to
429 *Acinetobacter baumannii* pathogenicity. Infect Immun 87(4):e00755-18
430 8. Jacobs AC, Hood I, Boyd KL, Olson PD, Morrison JM, Carson S, Sayood K, Iwen PC,
431 Skaar EP, Dunman PM. 2010. Inactivation of phospholipase D diminishes

432 *Acinetobacter baumannii* pathogenesis. Infect Immun 78:1952–1962.

433 9. Bentancor L V., Camacho-Peiro A, Bozkurt-Guzel C, Pier GB, Maira-Litran T. 2012.
434 Identification of Ata, a multifunctional trimeric autotransporter of *Acinetobacter*
435 *baumannii*. J Bacteriol 194:3950–3960.

436 10. Eijkelkamp BA, Stroeher UH, Hassan KA, Elbourne LDH, Paulsen IT, Brown MH. 2013.
437 H-NS plays a role in expression of *Acinetobacter baumannii* virulence features. Infect
438 Immun 81:2574.

439 11. Tipton KA, Dimitrova D, Rather PN. 2015. Phase-variable control of multiple
440 phenotypes in *Acinetobacter baumannii* strain AB5075. J Bacteriol 197:2593–2599.

441 12. Liou M-L, Soo P-C, Ling S-R, Kuo H-Y, Tang CY, Chang K-C. 2014. The sensor kinase
442 BfmS mediates virulence in *Acinetobacter baumannii*. J Microbiol Immunol Infect
443 47:275–281.

444 13. Cerqueira GM, Kostoulias X, Khoo C, Aibinu I, Qu Y, Traven A, Peleg AY. 2014. A global
445 virulence regulator in *Acinetobacter baumannii* and Its control of the phenylacetic
446 acid catabolic pathway. J Infect Dis 210:46–55.

447 14. Morris FC, Dexter C, Kostoulias X, Uddin MI, Peleg AY. 2019. The mechanisms of
448 disease caused by *Acinetobacter baumannii*. Front Microbiol 10:1601.

449 15. Rutherford ST, Bassler BL. 2012. Bacterial quorum sensing: its role in virulence and
450 possibilities for its control. Cold Spring Harb Perspect Med 2:a012427.

451 16. Williams P, Winzer K, Chan WC, Cámara M. 2007. Look who's talking: communication
452 and quorum sensing in the bacterial world. Philos Trans R Soc Lond B Biol Sci
453 362:1119–34.

454 17. Kamaraju S, Ch S, Ratnakar KS, Sritharan V. 2019. Quorum sensing system in
455 *Acinetobacter baumannii*: a potential target for new drug development. J Appl

456 Microbiol jam.14330.

457 18. Niu C, Clemmer KM, Bonomo RA, Rather PN. 2008. Isolation and characterization of
458 an autoinducer synthase from *Acinetobacter baumannii*. J Bacteriol 190:3386–92.

459 19. Anbazhagan D, Mansor M, Yan GOS, Md Yusof MY, Hassan H, Sekaran SD. 2012.
460 Detection of quorum sensing signal molecules and identification of an autoinducer
461 synthase gene among biofilm forming clinical isolates of *Acinetobacter* spp. PLoS One
462 7:e36696.

463 20. Clemmer KM, Bonomo RA, Rather PN. 2011. Genetic analysis of surface motility in
464 Acinetobacter baumannii. Microbiology 157:2534.

465 21. Bhuiyan MS, Ellett F, Murray GL, Kostoulias X, Cerqueira GM, Schulze KE, Mahamad
466 Maifiah MH, Li J, Creek DJ, Lieschke GJ, Peleg AY. 2016. *Acinetobacter baumannii*
467 phenylacetic acid metabolism influences infection outcome through a direct effect on
468 neutrophil chemotaxis. Proc Natl Acad Sci U S A 113:9599–604.

469 22. Fernandez-Garcia L, Ambroa A, Blasco L, Bleriot I, López M, Alvarez-Marin R,
470 Fernández-Cuenca F, Martinez-Martinez L, Vila J, Rodríguez-Baño J, Garnacho-
471 Montero J, Cisneros JM, Pascual A, Pachón J, Bou G, Smani Y, Tomás M. 2018.
472 Relationship between the quorum network (sensing/quenching) and clinical features
473 of pneumonia and bacteraemia caused by *A. baumannii*. Front Microbiol 9:3105.

474 23. Michalska K, Chhor G, Clancy S, Jedrzejczak R, Babnigg G, Winans SC, Joachimiak A.
475 2014. RsaM: a transcriptional regulator of *Burkholderia* spp. with novel fold. FEBS J
476 281:4293–4306.

477 24. Mattiuzzo M, Bertani I, Ferluga S, Cabrio L, Bigirimana J, Guarnaccia C, Pongor S,
478 Maraite H, Venturi V. 2011. The plant pathogen *Pseudomonas fuscovaginae* contains
479 two conserved quorum sensing systems involved in virulence and negatively

480 regulated by RsaL and the novel regulator RsaM. Environ Microbiol 13:145–162.

481 25. Uzelac G, Patel HK, Devescovi G, Licastro D, Venturi V. 2017. Quorum sensing and
482 RsaM regulons of the rice pathogen *Pseudomonas fuscovaginae*. Microbiology
483 163:765–777.

484 26. Chen R, Barphagha IK, Karki HS, Ham JH. 2012. Dissection of quorum-sensing genes in
485 *Burkholderia glumae* reveals non-canonical regulation and the new regulatory gene
486 *tofM* for toxoflavin production. PLoS One 7:e52150.

487 27. Le Guillouzer S, Groleau M-C, Déziel E. 2018. Two *rsaM* homologues encode central
488 regulatory elements modulating quorum sensing in *Burkholderia thailandensis*. J
489 Bacteriol 200(14):e00727-17.

490 28. Silja Inhülsen. 2011. Investigations of the quorum sensing circuitry in *Burkholderia*
491 *cenocepacia* H111. PhD thesis. University of Zürich, Zürich.

492 29. Jacobs AC, Thompson MG, Black CC, Kessler JL, Clark LP, McQueary CN, Gancz HY,
493 Corey BW, Moon JK, Si Y, Owen MT, Hallock JD, Kwak YI, Summers A, Li CZ, Rasko DA,
494 Penwell WF, Honnold CL, Wise MC, Waterman PE, Lesho EP, Stewart RL, Actis LA,
495 Palys TJ, Craft DW, Zurawski D V. 2014. AB5075, a highly virulent isolate of
496 *Acinetobacter baumannii*, as a model strain for the evaluation of pathogenesis and
497 antimicrobial treatments. MBio.

498 30. Mayer C, Muras A, Romero M, López M, Tomás M, Otero A. 2018. Multiple quorum
499 quenching enzymes are active in the nosocomial pathogen *Acinetobacter baumannii*
500 ATCC17978. Front Cell Infect Microbiol 8:310.

501 31. Ahlgren NA, Harwood CS, Schaefer AL, Giraud E, Greenberg EP. 2011. Aryl-
502 homoserine lactone quorum sensing in stem-nodulating photosynthetic
503 bradyrhizobia. Proc Natl Acad Sci U S A 108:7183–7188.

504

505 32. Gelencsér Z, Galbáts B, Gonzalez JF, Choudhary KS, Hudaiberdiev S, Venturi V, Pongor
506 S. 2012. Chromosomal arrangement of ahl-driven quorum sensing circuits in
507 *Pseudomonas*. ISRN Microbiol 2012:1–6.

508 33. Rampioni G, Schuster M, Greenberg EP, Bertani I, Grasso M, Venturi V, Zennaro E,
509 Leoni L. 2007. RsaL provides quorum sensing homeostasis and functions as a global
510 regulator of gene expression in *Pseudomonas aeruginosa*. Mol Microbiol 66:1557–
511 1565.

512 34. Bondí R, Longo F, Messina M, D'Angelo F, Visca P, Leoni L, Rampioni G. 2017. The
513 multi-output incoherent feedforward loop constituted by the transcriptional
514 regulators LasR and RsaL confers robustness to a subset of quorum sensing genes in
515 *Pseudomonas aeruginosa*. Mol Biosyst 13:1080–1089.

516 35. Wand ME, Bock LJ, Turton JF, Nugent PG, Sutton JM. 2012. *Acinetobacter baumannii*
517 virulence is enhanced in *Galleria mellonella* following biofilm adaptation. J Med
518 Microbiol 61:470–477.

519 36. Bhargava N, Sharma P, Capalash N. 2010. Quorum sensing in *Acinetobacter*: an
520 emerging pathogen. Crit Rev Microbiol 36:349–360.

521 37. Kang Y-S, Park W. 2010. Contribution of quorum-sensing system to hexadecane
522 degradation and biofilm formation in *Acinetobacter* sp. strain DR1. J Appl Microbiol
523 109:no-no.

524 38. Peleg AY, Jara S, Monga D, Eliopoulos GM, Moellering RC, Jr., Mylonakis E. 2009.
525 *Galleria mellonella* as a model system to study *Acinetobacter baumannii* pathogenesis
526 and therapeutics. Antimicrob Agents Chemother 53:2605.

527 39. Tomaras AP, Dorsey CW, Edelmann RE, Actis LA. 2003. Attachment to and biofilm

528 formation on abiotic surfaces by *Acinetobacter baumannii*: involvement of a novel
529 chaperone-usher pili assembly system. Microbiology 149:3473–3484.
530 40. Rumbo-Feal S, Gómez MJ, Gayoso C, Álvarez-Fraga L, Cabral MP, Aransay AM,
531 Rodríguez-Ezpeleta N, Fullaondo A, Valle J, Tomás M, Bou G, Poza M. 2013. Whole
532 transcriptome analysis of *Acinetobacter baumannii* assessed by RNA-sequencing
533 reveals different mRNA expression profiles in biofilm compared to planktonic cells.
534 PLoS One 8:e72968.
535 41. Pakharukova N, Tuittila M, Paavilainen S, Malmi H, Parilova O, Teneberg S, Knight SD,
536 Zavialov A V. 2018. Structural basis for *Acinetobacter baumannii* biofilm formation.
537 Proc Natl Acad Sci U S A 115:5558–5563.
538 42. Rumbo-Feal S, Pérez A, Ramelot TA, Álvarez-Fraga L, Vallejo JA, Beceiro A, Ohneck EJ,
539 Arivett BA, Merino M, Fiester SE, Kennedy MA, Actis LA, Bou G, Poza M. 2017.
540 Contribution of the *A. baumannii A1S_0114* gene to the interaction with eukaryotic
541 cells and virulence. Front Cell Infect Microbiol 7:108.
542 43. Gerdt JP, Wittenwyler DM, Combs JB, Boursier ME, Brummond JW, Xu H, Blackwell
543 HE. 2017. Chemical interrogation of LuxR-type quorum sensing receptors reveals new
544 insights into receptor selectivity and the potential for interspecies bacterial signaling.
545 ACS Chem Biol 12:2457–2464.
546 44. Gallagher LA, Ramage E, Weiss EJ, Radey M, Hayden HS, Held KG, Huse HK, Zurawski
547 D V, Brittnacher MJ, Manoil C. 2015. Resources for genetic and genomic analysis of
548 emerging pathogen *Acinetobacter baumannii*. J Bacteriol 197:2027–35.
549 45. Choi K-H, Gaynor JB, White KG, Lopez C, Bosio CM, Karkhoff-Schweizer RR, Schweizer
550 HP. 2005. A Tn*7*-based broad-range bacterial cloning and expression system. Nat
551 Methods 2:443–448.

552 46. Ortori CA, Dubern JF, Chhabra SR, Cámara M, Hardie K, Williams P, Barrett DA. 2011.
553 Simultaneous quantitative profiling of N-acyl-L-homoserine lactone and 2-alkyl-4(1H)-
554 quinolone families of quorum-sensing signaling molecules using LC-MS/MS. Anal
555 Bioanal Chem. 399:839-50.
556 47. Edgar RC. MUSCLE: multiple sequence alignment with high accuracy and high
557 throughput. 32:1792-1797
558 48. Robert X, Gouet P. 2014. Deciphering key features in protein structures with the new
559 ENDscript server. Nucleic Acids Res;42(Web Server issue):W320-W324.
560 49. Ng CK, How KY, Tee KK, Chan KG. 2019. Characterization and transcriptome studies of
561 autoinducer synthase gene from multidrug resistant *Acinetobacter baumannii* strain
562 863.*Genes (Basel)* 10(4):282
563 50. Edgar R, Domrachev M, Lash AE. 2002. Gene Expression Omnibus: NCBI gene
564 expression and hybridization array data repository. *Nucleic Acids Res* 30(1):207-10
565
566

567 **FIGURE LEGENDS**

568 **FIG 1 (A)** Schematic of the *abaRMI* quorum sensing locus in *A. baumannii* AB5075 showing
569 the organization of the three QS genes and their orientation. Green boxes represent
570 predicted *lux* boxes. Curved arrows represent the predicted *abaM* and *abaI* promoters. **(B)**
571 Multiple sequence alignment of *A. baumannii* AB5075 AbaM (Abau) with previously
572 characterized orthologs in other bacterial species: Bcen: *Burkholderia cenocepacia* J2315
573 *Bc*RsaM, Pfus: *Pseudomonas fuscovaginae* UPB0736 RsaM, Btha-2: *Burkholderia*
574 *thailandensis* E264
575 RsaM-2, Bglu: *Burkholderia glumae* BGR1 TofM, *Burkholderia thailandensis* E264 RsaM-1.
576 The MUSCLE algorithm (47) was used to create the alignment and ESPript (48) to render
577 residue similarities and generate the final figure. White characters in a red background
578 indicate conserved residues. Red residues indicate conservative substitutions. Blue frames
579 indicate highly conserved regions. The secondary structures in *B. cenocepacia Bc*RsaM (PDB
580 entry 4O2H) is displayed above the alignment. η: 3_{10}-helix, α: α-helices, β: β-strands, **TT**:
581 strict β-turns, **TTT**: strict α-turns.

582 **FIG 2** AHL production in wild-type, *abaI*::T26 and *abaM*::T26. **(A)** Chemical structures of the
583 AHLs produced by *A. baumannii* AB5075**.** Quantification of OHC12 **(B)** and OHC10 **(C)**
584 production throughout growth. Error bars represent the standard deviation between three
585 biological replicates. Asterisks indicate statistically significant differences: **, $p \leq 0.01$; ***,
586 $p \leq 0.001$

587

588 **FIG 3** Phenotypic characterization of the *Acinetobacter abaM* and *abaI* mutants**. (A)** Surface
589 motility on agar **(B)** Biofilm formation on polypropylene. For both biofilm and surface

590 motility assays, error bars indicate standard deviation. Asterisks indicate statistically
591 significant differences compared with the wild-type AB5075 strain: ***, $p \leq 0.001$; ****, $p \leq$
592 0.0001. **(C)** *Galleria mellonella* larvae killing after inoculation of approximately 2 x 10^4 (left)
593 or 2 x 10^5 (right) CFU/larva. Each graph represents data from 3 independent biological
594 replicates together. At least 30 larvae were used for each strain and assay. None of the
595 control larvae died after 5 days. Asterisks indicate statistically significant differences
596 compared with the wild-type AB5075 strain: ****, $p \leq 0.0001$.

597 **FIG 4** Comparison of the transcriptomes of the *abaI*::T26 and *abaM*::T26 mutants. Genes
598 differentially expressed in **(A)** *abaM*::T26 **(B)** *abaI*::T26 compared with wild-type. Blue
599 circles indicate upregulated genes. Red circles indicate downregulated genes. Grey circles
600 represent genes where changes in expression are unlikely to be biologically significant. **(C)**
601 Venn diagram showing that AbaM regulates genes that are both QS-dependent and QS-
602 independent.

603 **FIG 5** Validation ABUW_3773 and *csu* expression by quantitative real-time PCR**.** Relative
604 expression of *csuA/B* and *ABUW_3773* in mutants compared with the wild-type AB5075
605 strain. The expression was normalized in relation to an endogenous control gene (*rpoB*).
606 Error bars indicate standard deviation between 3 independent biological replicates.
607 Hashtags (#) indicate a biologically significant difference ($|\log2(\text{fold change})| \geq 1$)
608 compared to the wild-type.

609 **FIG 6** Expression of *abaM* and *abaI*. **(A)** *abaM* promoter activity in *A. baumannii* A5075 wild
610 type, *abaM*::T26 and *abaI*::T26 relative to the wild-type strain. **(B)** *abaM* promoter activity
611 in response to exogenous OHC12 as a function of growth (RLU/OD_{600}). (**C**) *abaI* promoter

612 activity in wild type, *abaI* mutant and in response to exogenous OHC12 as a function of
613 growth (RLU/OD_{600}). Error bars indicate standard deviation between 3 independent
614 biological replicates. Asterisks indicate statistically significant differences compared to the
615 wild-type AB5075 strain: ***, $p \leq 0.001$; ****, $p \leq 0.0001$.

616 **FIG 7. Proposed model for the QS/AbaM incoherent feed forward loop (IFFL) in *A.***
617 ***baumannii* 5075.** AbaR activated by OHC12 positively activates expression of *abaM* and *abaI*
618 and hence OHC12 production. AbaM is negatively autoregulated and also represses
619 expression of both *abaR* and *abaI*. Under the growth conditions used here, AbaM negatively
620 regulates surface motility, biofilm and Csu pili but is required for virulence as *abaM* mutants
621 are avirulent in *Galleria mellonella* larvae. Green arrows and red blunt ended lines represent
622 positive and negative regulation respectively
623

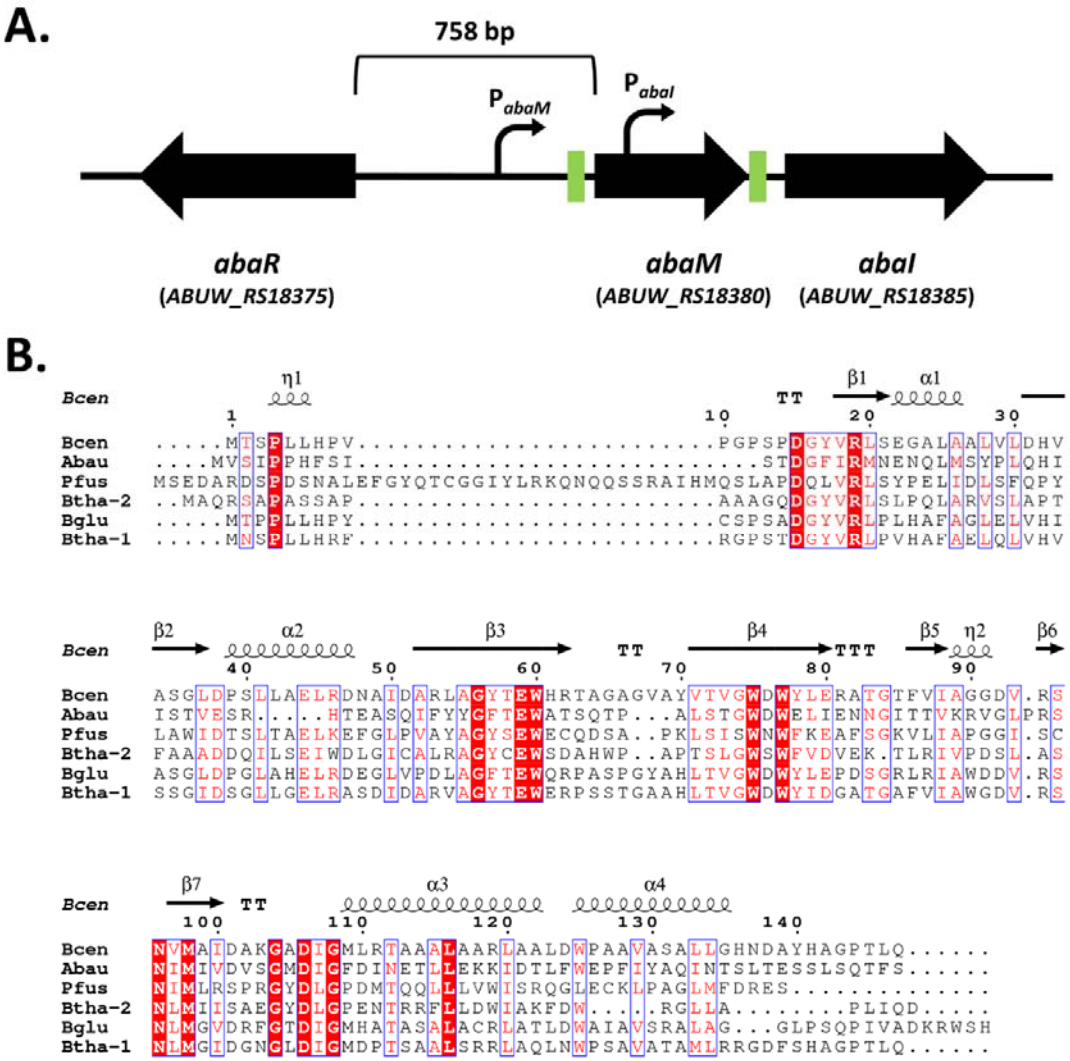

FIG 1 (A) Schematic of the *abaRMI* quorum sensing locus in *A. baumannii* AB5075 showing the organization of the three QS genes and their orientation. Green boxes represent predicted *lux* boxes. Curved arrows represent the predicted *abaM* and *abaI* promoters. **(B)** Multiple sequence alignment of *A. baumannii* AB5075 AbaM (Abau) with previously characterized orthologs in other bacterial species: Bcen: *Burkholderia cenocepacia* J2315 *Bc*RsaM, Pfus: *Pseudomonas fuscovaginae* UPB0736 RsaM, Btha-2: *Burkholderia thailandensis* E264 RsaM-2, Bglu: *Burkholderia glumae* BGR1 TofM, *Burkholderia thailandensis* E264 RsaM-1. The MUSCLE algorithm (47) was used to create the alignment

633 and ESPript (48) to render residue similarities and generate the final figure. White
634 characters in a red background indicate conserved residues. Red residues indicate
635 conservative substitutions. Blue frames indicate highly conserved regions. The secondary
636 structures in *B. cenocepacia Bc*RsaM (PDB entry 4O2H) is displayed above the alignment. η:
637 3_{10}-helix, α: α-helices, β: β-strands, **TT**: strict β-turns, **TTT**: strict α-turns.
638

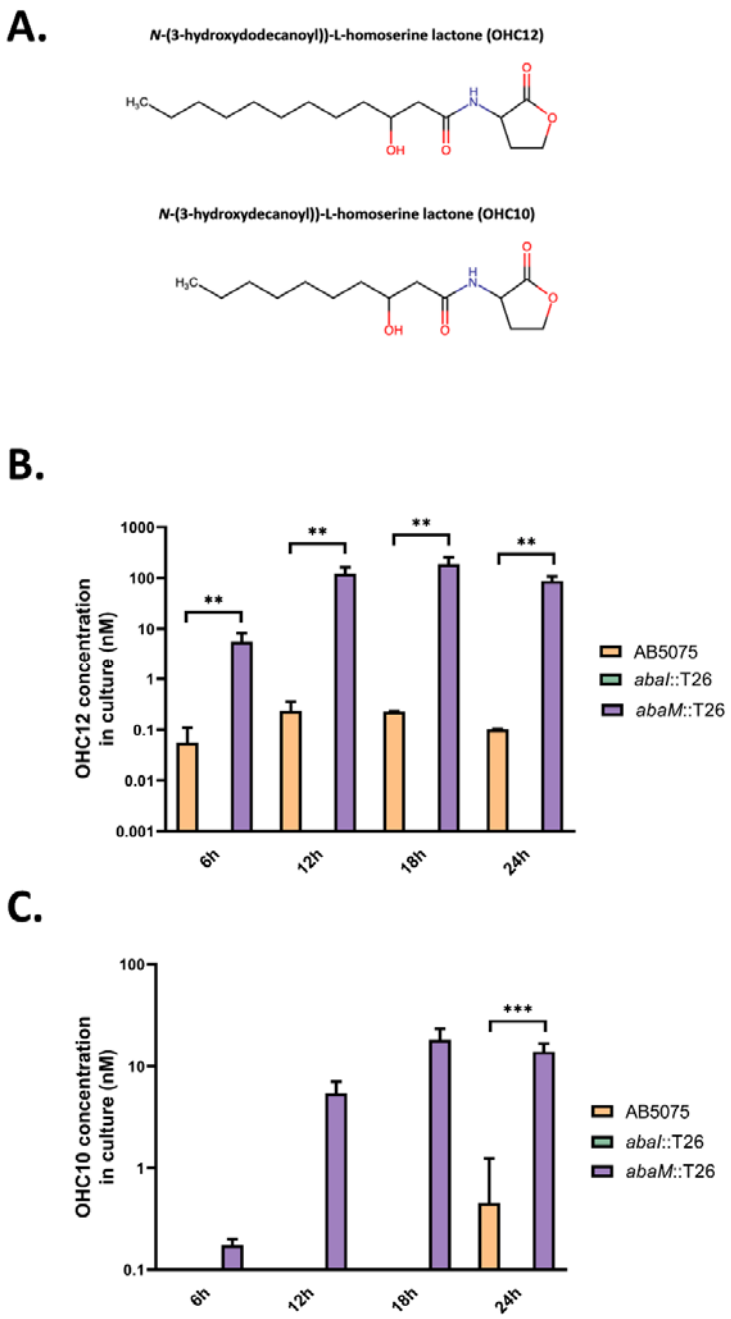

FIG 2 AHL production in wild-type, *abaI*::T26 and *abaM*::T26. **(A)** Chemical structures of the AHLs produced by *A. baumannii* AB5075**.** Quantification of OHC12 **(B)** and OHC10 **(C)** production throughout growth. Error bars represent the standard deviation between three biological replicates. Asterisks indicate statistically significant differences: **, $p \leq 0.01$; ***, $p \leq 0.001$.

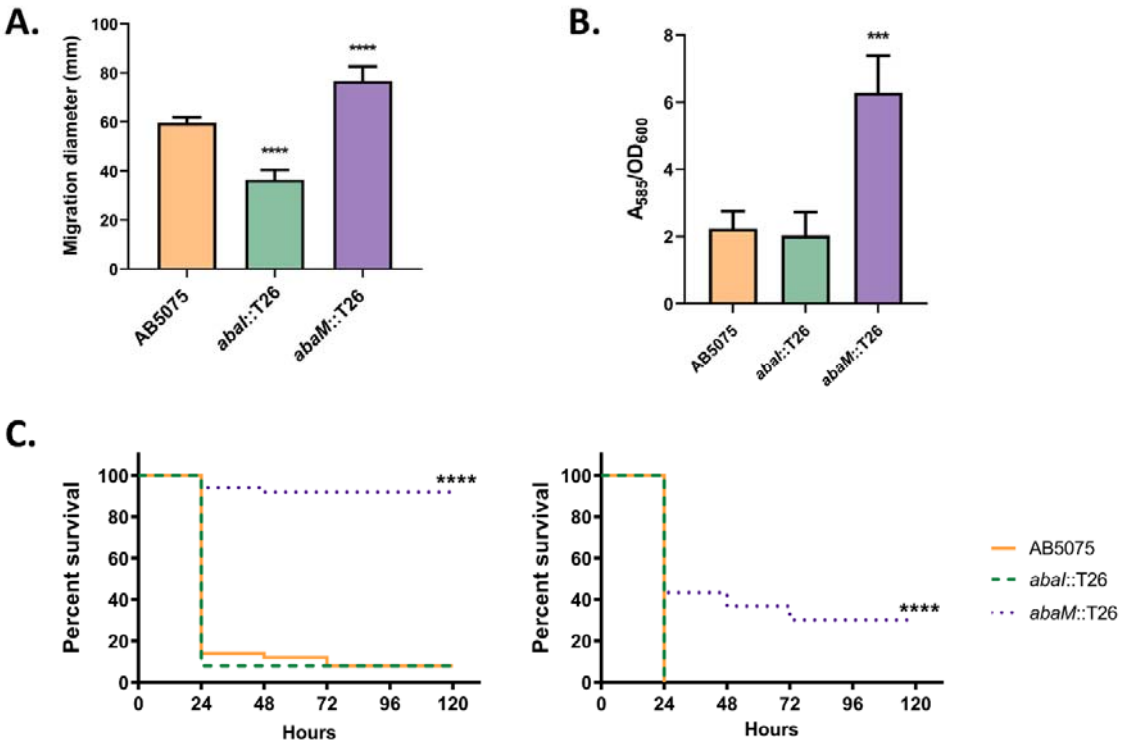

645

646 **FIG 3** Phenotypic characterization of the *Acinetobacter abaM* and *abaI* mutants. **(A)** Surface
647 motility on agar **(B)** Biofilm formation on polypropylene**.** For both biofilm and surface
648 motility assays, error bars indicate standard deviation. Asterisks indicate statistically
649 significant differences compared with the wild-type AB5075 strain: ***, $p \leq 0.001$; ****, $p \leq$
650 0.0001. **(C)** *Galleria mellonella* larvae killing after inoculation of approximately 2×10^4 (left)
651 or 2×10^5 (right) CFU/larva. Each graph represents data from 3 independent biological
652 replicates together. At least 30 larvae were used for each strain and assay. None of the
653 control larvae died after 5 days. Asterisks indicate statistically significant differences
654 compared with the wild-type AB5075 strain: ****, $p \leq 0.0001$.

655

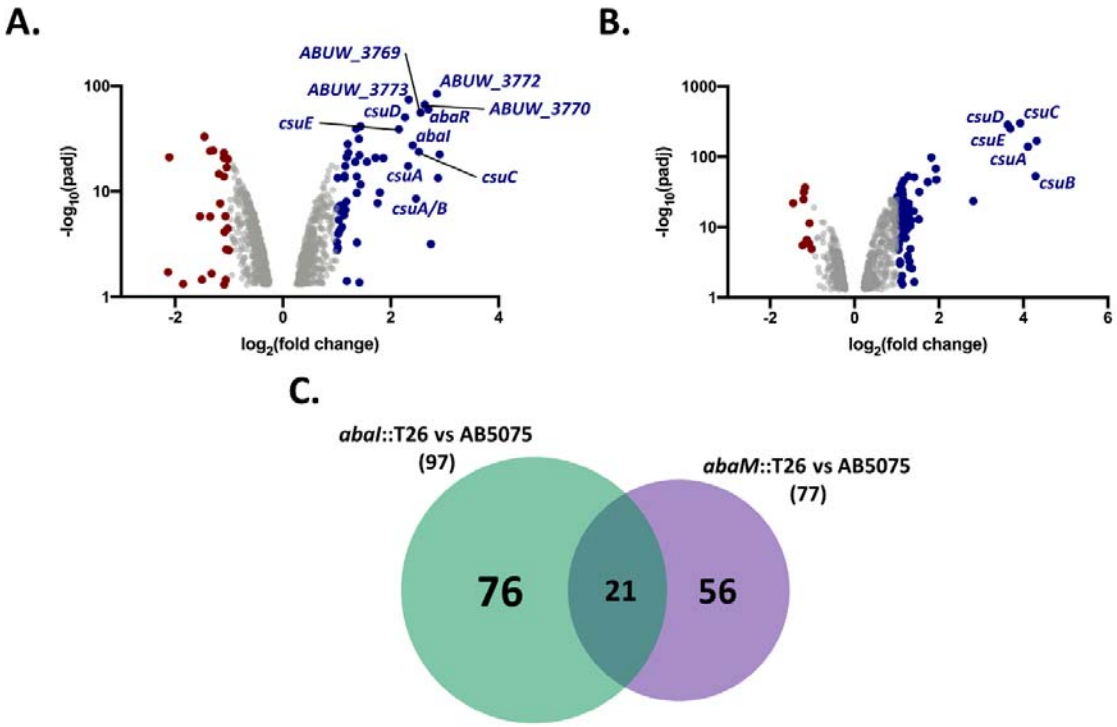

FIG 4 Comparison of the transcriptomes of the *abaI*::T26 and *abaM*::T26 mutants. Genes differentially expressed in **(A)** *abaM*::T26 or **(B)** *abaI*::T26 compared with wild-type. Blue circles indicate upregulated genes. Red circles indicate downregulated genes. Grey circles represent genes where changes in expression are unlikely to be biologically significant. **(C)** Venn diagram showing that AbaM regulates genes that are both QS-dependent and QS-independent.

664

665

666

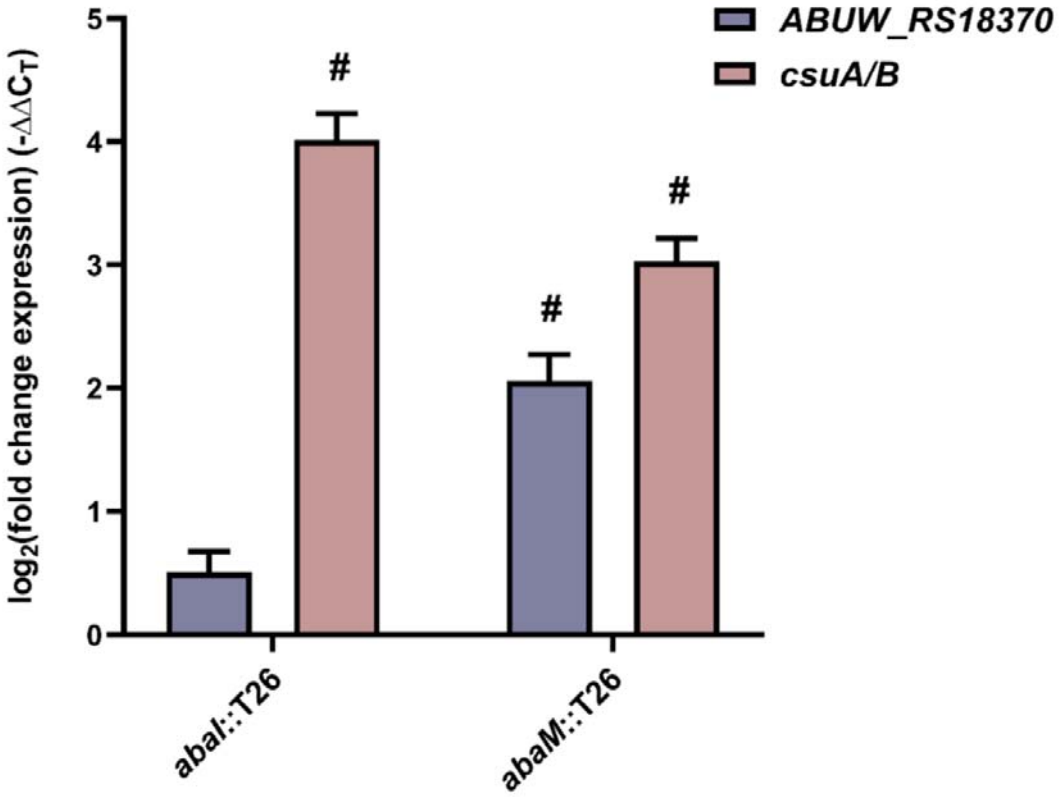

667

668 **FIG 5** Validation ABUW_3773 and *csu* expression by quantitative real-time PCR. Relative
669 expression of *csuA/B* and *ABUW_3773* in *abaI*::T26 and *abaM*::T26 mutants compared with
670 the wild-type AB5075 strain. The expression was normalized in relation to an endogenous
671 control gene (*rpoB*). Error bars indicate standard deviation between 3 independent
672 biological replicates. Hashtags (#) indicate a biologically significant difference (|log2(fold
673 change)| ≥ 1) compared to the wild- type.

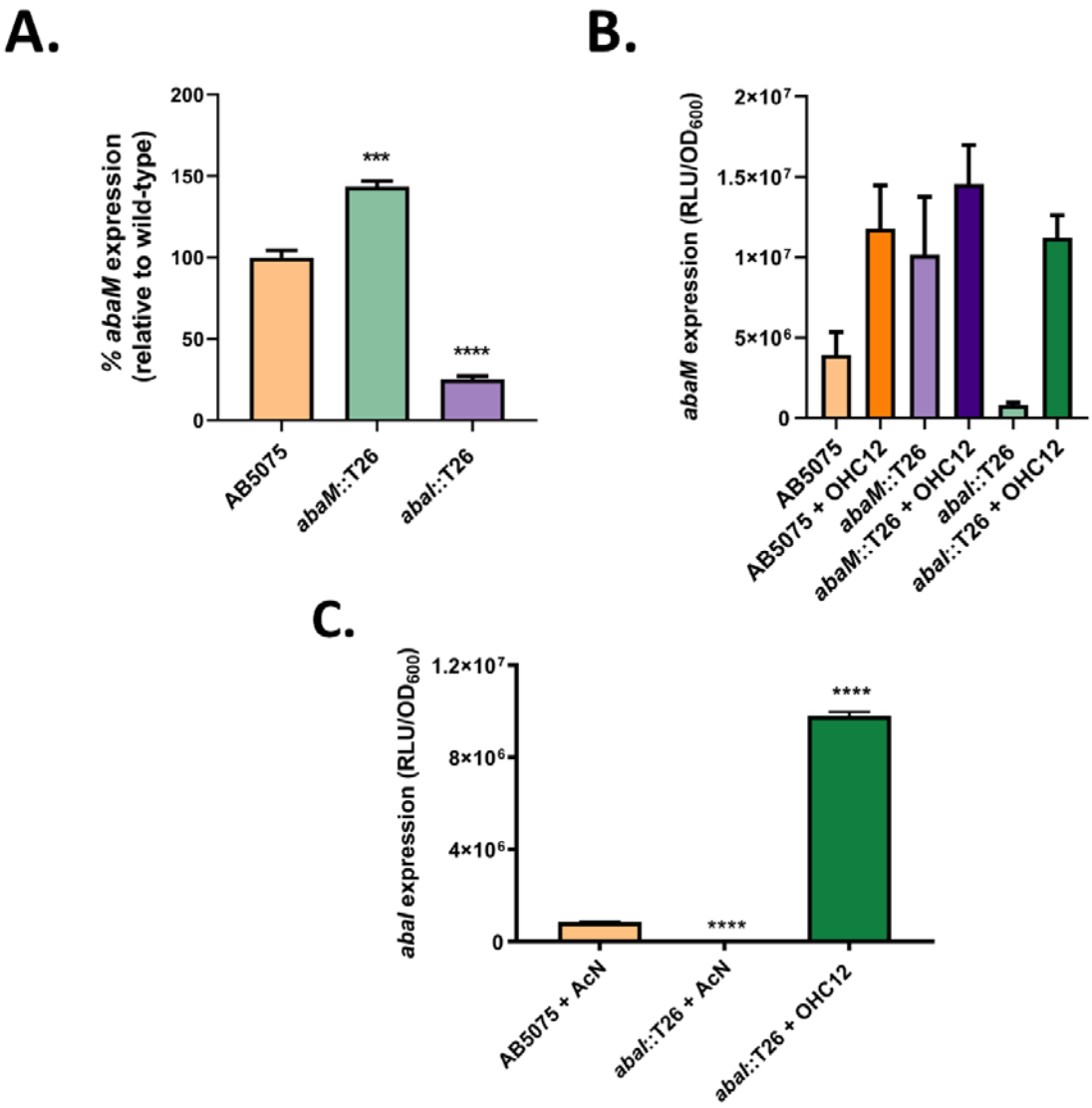

FIG 6 Expression of *abaM* and *abaI*. **(A)** *abaM* promoter activity in *A. baumannii* A5075 wild type, *abaM*::T26 and *abaI*::T26 relative to the wild-type strain. **(B)** *abaM* promoter activity in response to exogenous OHC12 (200 nM) as a function of growth (RLU/OD_{600}). (**C**) *abaI* promoter activity in wild type, *abaI* mutant and in response to exogenous OHC12 as a function of growth (RLU/OD_{600}). Acn, acetonitrile solvent control. Error bars indicate standard deviation between 3 independent biological replicates. Asterisks indicate statistically significant differences compared to the wild-type AB5075 strain: ***, $p \leq 0.001$; ****, $p \leq 0.0001$.

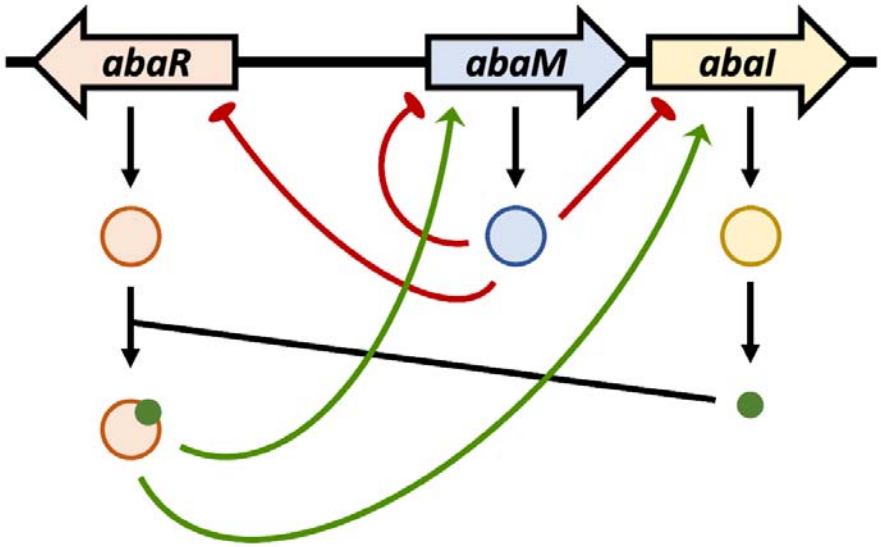

684

685 **FIG 7 Proposed model for the QS/AbaM incoherent feed forward loop (IFFL) in *A.***
686 ***baumannii* 5075.** AbaR activated by OHC12 positively activates expression of *abaM* and *abaI*
687 and hence OHC12 production. AbaM is negatively autoregulated and also represses
688 expression of both *abaR* and *abaI*. Under the growth conditions used here, AbaM negatively
689 regulates surface motility, biofilm and Csu pili but is required for virulence as *abaM* mutants
690 are avirulent in *Galleria mellonella* larvae. Green arrows and red blunt ended lines represent
691 positive and negative regulation respectively.